atmosphere

Article

Climate Change Effects through MFDFA Study of Temperature in Serbia

Tatijana Stosic [1], Borko Stosic [1], Milica Tošić [2], Irida Lazić [2], Vladimir Djurdjević [2] and Ivana Tošić [2,*]

[1] Departamento de Estatística e Informática, Universidade Federal Rural de Pernambuco, Rua Dom Manoel de Medeiros s/n, Dois Irmãos, Recife 52171-900, Brazil; tastosic@gmail.com (T.S.); borkostosic@gmail.com (B.S.)
[2] Institute for Meteorology, Faculty of Physics, University of Belgrade, 11000 Belgrade, Serbia; milica.tosic@ff.bg.ac.rs (M.T.); irida.lazic@ff.bg.ac.rs (I.L.); vdj@ff.bg.ac.rs (V.D.)
* Correspondence: itosic@ff.bg.ac.rs

Abstract: We investigate multifractal properties of daily means of air temperature over the territory of Serbia, by using Multifractal detrended fluctuation analysis. Temperature anomalies in two periods 1961–1990 and 1991–2020 are calculated from the E-OBSv26.0e gridded dataset with 0.10° (~12 km) resolution, totaling 1278 daily temperature series for each period. The MFDFA parameters: position of the maximum of the spectrum α_0, width of the spectrum W and asymmetry r, obtained from the total of 2556 MFDFA runs are interpolated to yield their spatial distribution across Serbia in the two periods. We found several patterns in both the spatial distribution, and changes from first to second period. All series showed multifractal properties with overall persistent long-term correlations ($\alpha_0 > 0.5$) and the dominance of small fluctuations ($r > 0$). The persistence is weaker (smaller α_0 values) and multifractality is stronger (larger width W) in southern mountainous regions. In the second period the values of α_0 increased indicating stronger persistence of temperature dynamics, while multifractality became stronger (larger W) in northern region and weaker (smaller W) in southern region. In both periods the contribution to multifractality was dominated by small fluctuations ($r > 0$) that become stronger in the second period, indicated by the increase of the values of r over most of the country's area. These changes in the values of multifractal parameters indicate the increase of complexity of temperature dynamics in the second 30 years period which could be related to climate change.

Keywords: air temperature; time series; multifractal analysis; spatial interpolation

check for updates

Citation: Stosic, T.; Stosic, B.; Tošić, M.; Lazić, I.; Djurdjević, V.; Tošić, I. Climate Change Effects through MFDFA Study of Temperature in Serbia. *Atmosphere* **2023**, *14*, 1532. https://doi.org/10.3390/atmos14101532

Academic Editor: Graziano Coppa

Received: 11 September 2023
Revised: 3 October 2023
Accepted: 4 October 2023
Published: 6 October 2023

1. Introduction

The complexity of climate system emerges as the result of multiple interactions between many different components [1]. Climate variables such as temperature, precipitation and wind exhibit temporal and spatial fluctuations over wide range of scales as a result of complex nonlinear underlying processes which understanding requires the use of new concepts such as chaos theory [2,3], fractals and multifractals [4–8], information content [9,10] and complex networks [11,12]. The knowledge of these properties has shown useful for development and validation of new more reliable climate models on local and regional scales [13–15]. Multifractality of atmospheric processes is well known and documented in scientific literature [16]. Multifractal dynamics is found in time series of air temperature [17–19], rainfall [20–23] humidity [24], wind speed [25–27], solar radiation [28,29] and global climate indices [30,31]. Air temperature and precipitation are the principal variables used in detection of climate change [32] which is considered the most challenging problem in climate studies due to increased evidence of the influence of anthropogenic factors [33,34].

With the objective to contribute to better understanding of climate variability and climate change in this work we investigate the multifractal dynamics of daily temperature in Serbia, its spatial distribution, and the degree of change between two standard normal periods of 30 years. We apply Multifractal Detrended Fluctuation Analysis (MDFA) [35] to long term (1961–2020) high resolution gridded dataset of daily temperature over Serbia and calculate multifractal parameters (that quantify the position of maximum, width, and asymmetry of multifractal spectrum) which are related to different properties of temperature fluctuations (persistence, degree of multifractality and dominance of small/large fluctuations). By comparing the spatial distribution of these parameters over Serbia for two periods of 30 years (1961–1990 and 1991–2020) we investigate how possible climate change affects temperature fluctuations. Previous studies on air temperature in Serbia include analysis of annual and seasonal temperature trends [36], trends of extreme temperature indices [37–40] and analysis of cold and heat waves [41]. Bajat et al. [36] analyzed mean annual and seasonal temperature series in Serbia based on monthly data from 64 stations recorded over the period 1961–2010. For most stations they identified 1989 as change year and found that mean annual temperature displayed significant negative trend for 10 stations before change year, and positive significant trend for almost all stations after the change year. By analyzing trends of seasonal temperature, they found that the summer season had the largest contribution to annual trends. Unkašević and Tošić [39] analyzed the trends of six climate indices based on 61 years (1949–2009) of daily maximum and minimum temperature from 15 stations distributed across Serbia. They found the warmer tendency of Serbian climate with the most significant trends in the summer season. Ruml et al. [37] analyzed trends of 18 indices based on daily maximum and minimum temperature recorded in 26 stations during the period 1961–2010. They compared the results for two sub-periods (1961–1980 and 1981–2010) and found that hot indices exhibited cooling tendency in the first sub-period and warming tendency in the second sub-period, while cold indices displayed warming tendency over entire period. Recently, Tošić et al. [40] performed the comprehensive analysis of changes in mean and extreme temperature indices in Serbia using same high resolution daily gridded temperature dataset during the period of 1951–2020. They found increasing trend for both, mean maximum temperature and mean minimum temperature, all indices based on maximum temperature, while among indices based on minimum temperature, negative trend was found for cool days and cool nights. They also analyzed correlation between temperature indices and large-scale circulation patterns and found that East Atlantic (EA) pattern was strongly correlated with temperature indices (positive correlation with warm indices and negative correlation with cold indices).

Considering this evidence of climate change in Serbia which is in agreement with results obtained on global and European scale, in this work we performed multifractal analysis (using MFDFA) on 1278 daily temperature series from a high-resolution gridded dataset E-OBS. This is the first study using MFDFA in this part of Europe. We analyzed two sub-periods (1961–1990 and 1991–2020) that totals 2556 MFDFA runs which produced the spatial distribution of multifractal parameters for each sub-period. We investigate the relation of these parameters with terrain topology and changes from first to second sub-period. We also compare our results with the results of studies for other countries

2. Data and Methodology

2.1. Study Area and Dataset

Serbia is continental country located on the Balkan Peninsula, in the southeast of Europe, within the temperate climate zone between latitudes 41°50′ and 46°10′ N (Figure 1). Its relief gradually changes from northern part with flat and low elevation terrain situated within Pannonian plain, toward central and southern part which is covered by hills and mountains surrounding river valleys. The climate varies from moderate continental in northern part to continental in central part and modified Mediterranean in southern and southwestern part due to Mediterranean influence which is modified because the Dinaric Mountain range (that stretches through the west and southwest of the country) prevent humid air masses to move in from west [36,42]. The mean annual temperature varies between 3 °C in regions with altitude above 1500 m and 12 °C in the lowlands. The mean annual rainfall increases with altitude: 600 mm in northern region and between 800 mm and 1000 mm in the mountainous region [38].

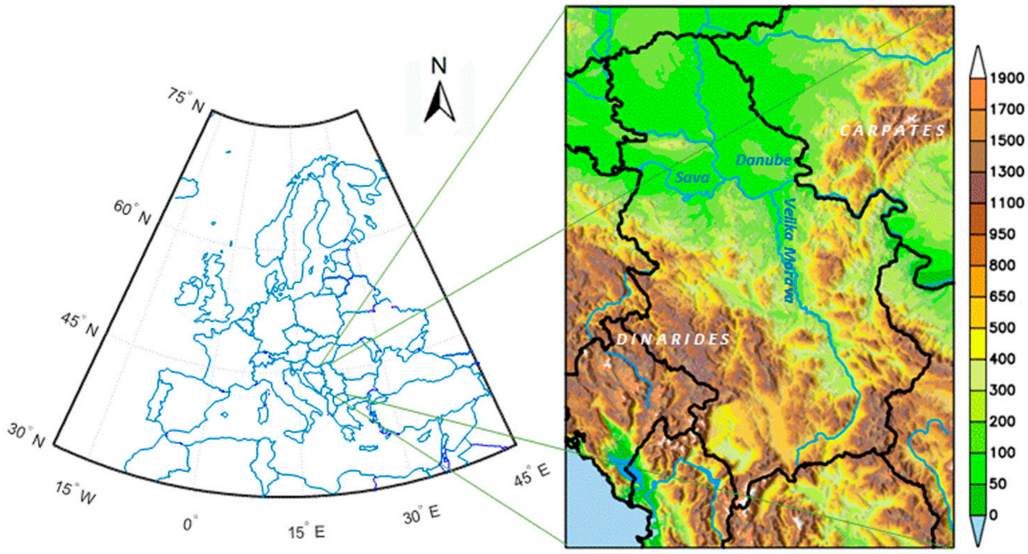

Figure 1. Position of Serbia in Europe (**left**) and map of Serbia with orography (**right**).

In this work we used the data from the E-OBS gridded dataset version 26.0e, for daily mean temperature (TG), with a horizontal resolution of 0.1°, for the period of 1961–2020. The E-OBS dataset represents one of the most comprehensive datasets for Europe, obtained by interpolating the collection of available station data [43]. The validation of temperature data for Serbia is performed by calculating the following scores: Bias, Mean Absolute Error (MAE), Root Mean Square Error (RMSE) and Correlation Coefficient (CC). Scores are calculated using daily observations from 57 stations and daily temperature from E-OBS dataset. We obtained a good agreement between the mean annual observed temperature (10.7 °C) and temperature from EOBS data (10.2 °C), as well as a Bias (−0.47), MAE (0.93), RMSE (1.12) and CC (0.99).

2.2. Multifractal Detrended Fluctuation Analysis

Fractal processes are characterized by a single scaling exponent that characterizes long-term correlations in terms of persistence (if large fluctuations are more likely to be followed by large fluctuations, and small fluctuations by other small fluctuations) or antipersistance (if large fluctuations are more likely to be followed by small fluctuations, and vice versa). A multifractal time series can be understood as a composition of interwoven subsets with small and large fluctuations that scale differently, and the analysis of long-term correlations requires a hierarchy of scaling exponents [35]. Multifractal analysis of temporal series has been addresses using different methods, such as wavelet transform modulus maxima (WTMM) method [44], multifractal detrended fluctuation analysis (MF-DFA) method [35] and multifractal detrending moving average method (MF-DMA) [45]. In this work we employ MF-DFA that was shown to produce reliable results [46] and has been widely used to analyze physiological signals [47], geophysical data [48], weather data [49], hydrological records [50], and financial time series [51].

The implementation of the MF-DFA algorithm goes as follows [35]. The first step is usually the integration of original fluctuation series $x(i)$, $i = 1, \ldots, N$, in order to produce the "profile"

$$X(k) = \sum_{i=1}^{k} [x(i) - \langle x \rangle],\ k = 1, \ldots, N$$

where $\langle x \rangle = \frac{1}{N}\sum_{i=1}^{k} x(i)$ is the average. If the original series represents random fluctuations, integrating the series produces a "profile" that increases as square root of "time" (index k), and departure from this square root behavior is the object of this analysis.

Next, the profile $X(k)$ is divided into $\lfloor N/n \rfloor$ non-overlapping segments of length n starting from $X(1)$ (here $\lfloor \cdot \rfloor$ stands the floor function), and another $\lfloor N/n \rfloor$ segments of size n starting from $X(N - n\lfloor N/n \rfloor + 1)$, so that the last segment ends at $X(N)$ (to account for the end of the series), the total number of segments now being $N_n = 2\lfloor N/n \rfloor$. In each segment $\nu = 1, \ldots, N_n$ the local trend $X_{n,\nu}(k)$ (linear or higher order polynomial least square fit) is estimated and subtracted from $X(k)$ to calculate the detrended variance

$$F^2(n,\nu) = \frac{1}{n}\sum\nolimits_{k=(\nu-1)n+1}^{\nu n} [X(k) - X_{n,\nu}(k)]^2$$

for each segment. Finally, an independent parameter q that can assume any real value except zero is introduced to find the so called qth order fluctuation function

$$F_q(n) = \left\{ \frac{1}{N_n} \sum\nolimits_{\nu=1}^{N_n} \left[F^2(n,\nu)\right]^{q/2} \right\}^{1/q}.$$

Parameter q serves as a "magnifying glass", where positive values of q enhance large fluctuations, and negative values enhance small fluctuations. Consider for example two segments where fluctuation $F(n,\nu_1) \equiv \left[F^2(n,\nu_1)\right]^{1/2}$ of the first segment has twice the magnitude of the fluctuation $F(n,\nu_2)$ of the second segment. Then, for $q = 10$ the contribution in the above sum $\left[F^2(n,\nu_1)\right]^{q/2}$ of the segment ν_1 is 1024 times larger than that of ν_2, and for $q = -10$ the role is reversed: contribution of ν_1 is 1024 times smaller than that of ν_2.

This calculation is repeated for different box sizes to provide the relationship between fluctuation function $F_q(n)$ and box size n. If long-term correlations are present, $F_q(n)$ increases with n according to a power law $F_q(n) \sim n^{h(q)}$, and the scaling exponent $h(q)$ is obtained as the slope of the linear regression of $\log F_q(n)$ versus $\log n$. This power law exponent $h(q)$ is called the generalized Hurst exponent, and for stationary time series $h(2)$ corresponds to the well-known Hurst exponent H [52,53]. As shown in the above example, $h(q)$ describes the scaling behavior of large fluctuations for positive values of q, and it describes the scaling behavior of small fluctuations for negative values of q. For monofractal time series there is a single scaling exponent so that $h(q)$ is a constant independent of q, while for multifractal time series $h(q)$ is a decreasing function of q.

Generalized Hurst exponent $h(q)$ are related to the Renyi exponent $\tau(q)$ defined by the standard partition function-based multifractal formalism as $\tau(q) = qh(q) - 1$. For monofractal signals $\tau(q)$ is a linear function of q (as $h(q) = const.$), and for multifractal signals $\tau(q)$ is a nonlinear function of q. It is often more convenient to characterize a multifractal process by the singularity spectrum $f(\alpha)$ which is related to $\tau(q)$ through the Legendre transform

$$\alpha(q) = \frac{d\tau(q)}{dq},$$

$$f(\alpha(q)) = q\alpha(q) - \tau(q),$$

where $f(\alpha)$ is the fractal dimension of the support of singularities with Lipschitz-Holder exponent α. The singularity spectrum of a monofractal signal is represented by a single point in the $f(\alpha)$ plane, whereas multifractal process yields a single humped function

Multifractal spectrum reflects the level of complexity of the underlying stochastic process and can be characterized by a set of three parameters: (i) the position of maximum α_0, (ii) width of the spectrum $W = \alpha_{max} - \alpha_{min}$, and (iii) the skew parameter $r = (\alpha_{max} + \alpha_{min} - 2\alpha_0)/(\alpha_{max} - \alpha_{min})$ [54,55], where $r = 0$ for symmetric shapes, $0 < r \leq 1$ for right-skewed shapes, and $-1 \leq r < 0$ for left-skewed shapes. If $\alpha_0 > 0.5$, the underlying process is overall persistent (larger value of α_0 indicates stronger persistency), and if $\alpha_0 < 0.5$ the process is overall antipersistent (smaller value of α_0 indicates stronger antipersistency). The width W of the spectrum measures the degree of multifractality of the process (the wider the range of the fractal exponents, the "richer" the structure of the process). The skew parameter r indicates which fractal exponents are dominant. If $f(\alpha)$ spectrum is right-skewed $(r > 0)$ the process is characterized by "fine structure" (large scaling exponents describing small fluctuations), and if the $f(\alpha)$ spectrum is left-skewed $(r < 1)$ the process is dominated by the scaling of large fluctuations (small scaling exponents). In summary, a signal with a high value of α_0, a wide range W of fractal exponents (higher degree of multifractality), and a right-skewed shape ($r > 0$) may be considered more complex than those with opposite characteristics [54].

To deal with a large number of MFDFA runs necessary for the current analysis, we have developed an optimized program in C language.

3. Results and Discussion

Descriptive statistics (mean and standard deviation) was calculated for all 1278 grid cells, interpolated and presented on Figure 2.

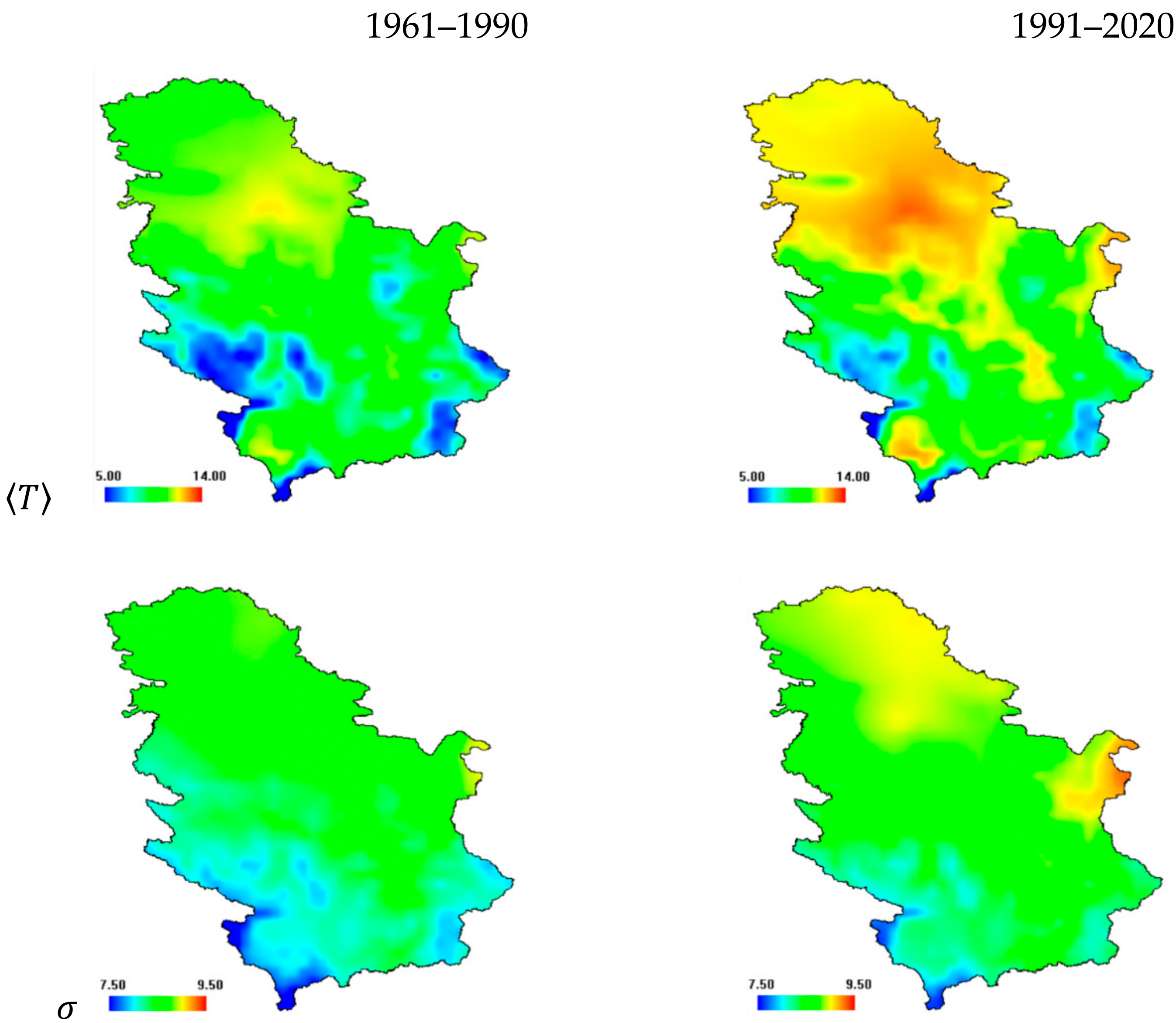

Figure 2. Mean temperature (top row) and corresponding standard deviation (bottom row) for the two considered periods: 1961–1990 (left column) and 1991–2020 (right column).

The mean annual temperatures between 9 and 11 °C prevailed in Serbia during the period 1961–1990 (Figure 2). The highest temperatures (around 12 °C) are recorded in the wider Belgrade area, and in valleys along the Sava and Velika Morava River (Figure 1), from 1961 to 1990. The lowest temperatures, below 6 °C, are observed in the mountain regions of southwestern and southeastern Serbia. The region with the lowest temperatures retained only at the mountains in southwestern Serbia during the period 1991–2020 (Figure 2). Mean annual temperatures between 9 and 11 °C are recorded in central and southern Serbia from 1991 to 2020. Temperatures above 11.5 °C prevailed in northern and eastern Serbia, and along Velika Morava River. The highest temperatures above 13 °C are recorded in the wider Belgrade area from 1991 to 2020.

Like a mean temperature, a standard deviation increased in Serbia in the second considered period (1991–2020). A standard deviation in value of 8 °C prevailed in Serbia during the period 1961–1990. The lowest values (7.5 °C) are recorded in southwestern Serbia, while the highest one at the far east (Figure 2). During the second period (1991–2020), values of standard deviation were above 8 °C in the wider Belgrade area and northern Serbia, with the highest values above 9 °C at the far east of Serbia (Figure 2).

3.1. Multifractal Analysis

The MFDFA method was applied on deseasonalized series (anomalies). For the two periods 1961–1990 and 1991–2020, for each calendar day i temperature anomalies are calculated as $z_{i,j} = \left(x_{i,j} - \mu_i\right)/\sigma_i$, where $x_{i,j}$ is mean temperature on day i of year j of the period, μ_i is the mean and σ_i is standard deviation over the years of the period. We applied MFDFA method on anomaly temporal series for all the 1278 grid cells for the two periods (1961–1990 and 1991–2020), totaling 2556 MFDFA runs using the range of q from -10 to +10, with a step of 0.1. The multifractal spectrum for a sample grid point at latitude 44.15 and longitude 21.35, corresponding to the central Serbia region close to the city of Kragujevac for the period 1961–1990, is shown in Figure 3 together with the corresponding spectrum for shuffled anomaly series. The shuffling procedure used implements 10,000$\times$ N transpositions (N = 10,957) and was repeated here 100 times with different random number generator seeds in order to obtain the mean and standard deviation. The fact that the spectrum for shuffled data becomes narrower and is shifted leftwards, centered about $\alpha = 0.5$ demonstrates that the observed multifractality is mainly due to long-range correlations, rather than to a broad probability density function [35].

The spatial distribution of multifractal parameters of over the Serbian territory for two periods (1961–1990 and 1991–2020) is shown in Figure 4 where we observed following patterns. The temperature series exhibit long-term persistent correlations (α_0> 0.5), with weaker persistence (lower α_0 value) in mountainous regions with higher elevation (western and southeastern regions, Figure 1) and lower temperature (Figure 2). In the second period when the temperature increased in all regions, the values of α_0 also increased indicating that temperature dynamics become more persistent. Putniković [56], applying an objective classification scheme of atmospheric circulation over Serbia, pointed out that the anticyclonic weather type, which is the most persistent circulation type, dominated in all seasons with a positive trend except for autumn. The width W of the spectrum also shows marked spatial variability: larger width (higher degree of multifractality) in mountainous regions (southern part, Figure 1) that decreased in the second period indicating loss of "richness" in scaling exponents of temperature fluctuations and consequently weaker multifractality. In northern parts with lower elevations, the multifractality of temperature series become stronger in the second period indicated by the increase of spectrum width. Thus contrary of what was observed for α_0 for which the direction of change from the first to second period was consistent (increasing) for all regions preserving the north-south gradient (higher α_0 values in northern part), the clear positive north-south gradient of W values that was observed in the first period was inverted in the second period: the width of the spectrum decreased from northern to central region and then increased in southern region, but it is still lower than in norther part. These changes can be better understood by analyzing skew parameter r. The values of r are positive indicating that small fluctuations contribute more to the multifractality of the process. In the second period these values stay positive and become larger in northern and smaller in central regions following the change of the width of $f(\alpha)$ spectrum. This indicates that the change in the width of the spectrum in these areas is due to the change in the dominance of small fluctuations (described by the right side of the spectrum). In the southern region the width of the spectrum decreased while the skew parameter increased, indicating that while dominance of small fluctuations become stronger widening the right side of $f(\alpha)$ spectrum in the second period, the contribution of large fluctuations to multifractality of temperature series (described by left side of the spectrum) become weaker, leading to the overall shorter spectrum width and lower degree of multifractality. Considering that a signal with a high value of α_0, a wide range W of fractal exponents (higher degree of multifractality), and a right-skewed shape ($r > 0$) may be considered more complex than those with opposite characteristics [52], the observed changes of multifractal parameters (Figure 4) indicated that in the second period overall complexity of temperature series increased in northern part of country, and decreased in southern part. Mimić et al. [57] analyzed the complexity of daily maximum and minimum temperature and daily precipitation from seven station on Serbia (recorded during the period 1951–2010) using information theory measures Kolmogorov complexity and Sample entropy. They found that for all stations both measures (calculated for 1year periods) exhibit positive trend for maximum temperature indicating the increase in complexity. The results of the multifractal analysis of mean temperature in Serbia from 1278 grid cells of E-OBS dataset also indicate the increase in complexity in northern part of the country.

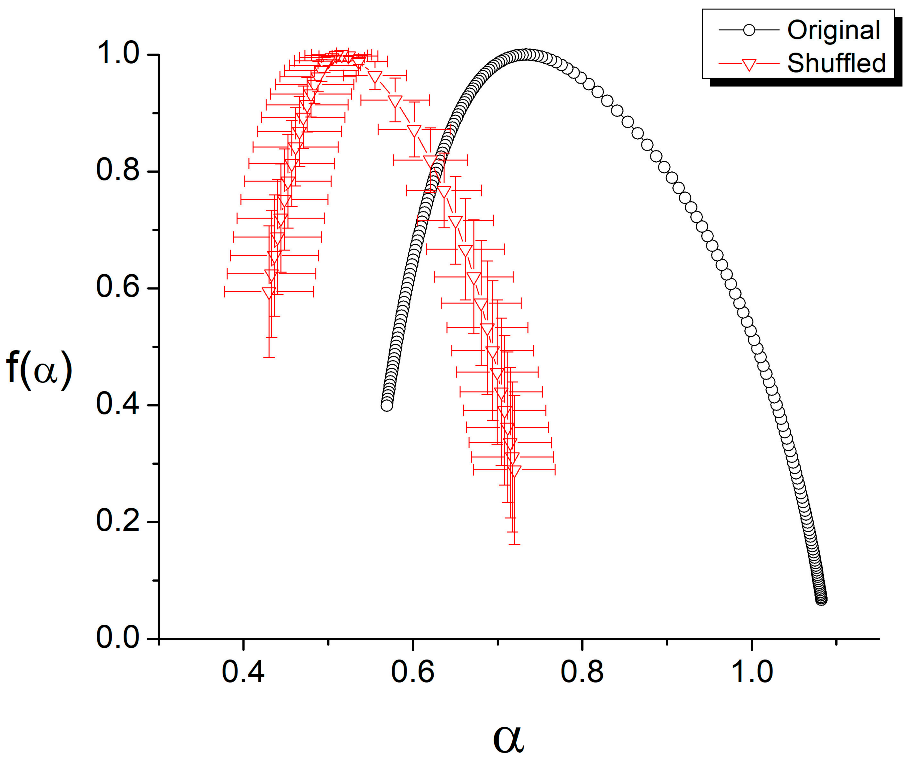

Figure 3. Multifractal spectra for the original and the shuffled anomaly series for a sample grid point at latitude 44.15 and longitude 21.35, corresponding to the central Serbia region close to the city of Kragujevac. The shuffled spectra correspond to mean values for 100 surrogate shuffled series, and the error bars to plus minus two standard deviations (the q parameter resolution was reduced here $\Delta q = 0.5$ for better visualization).

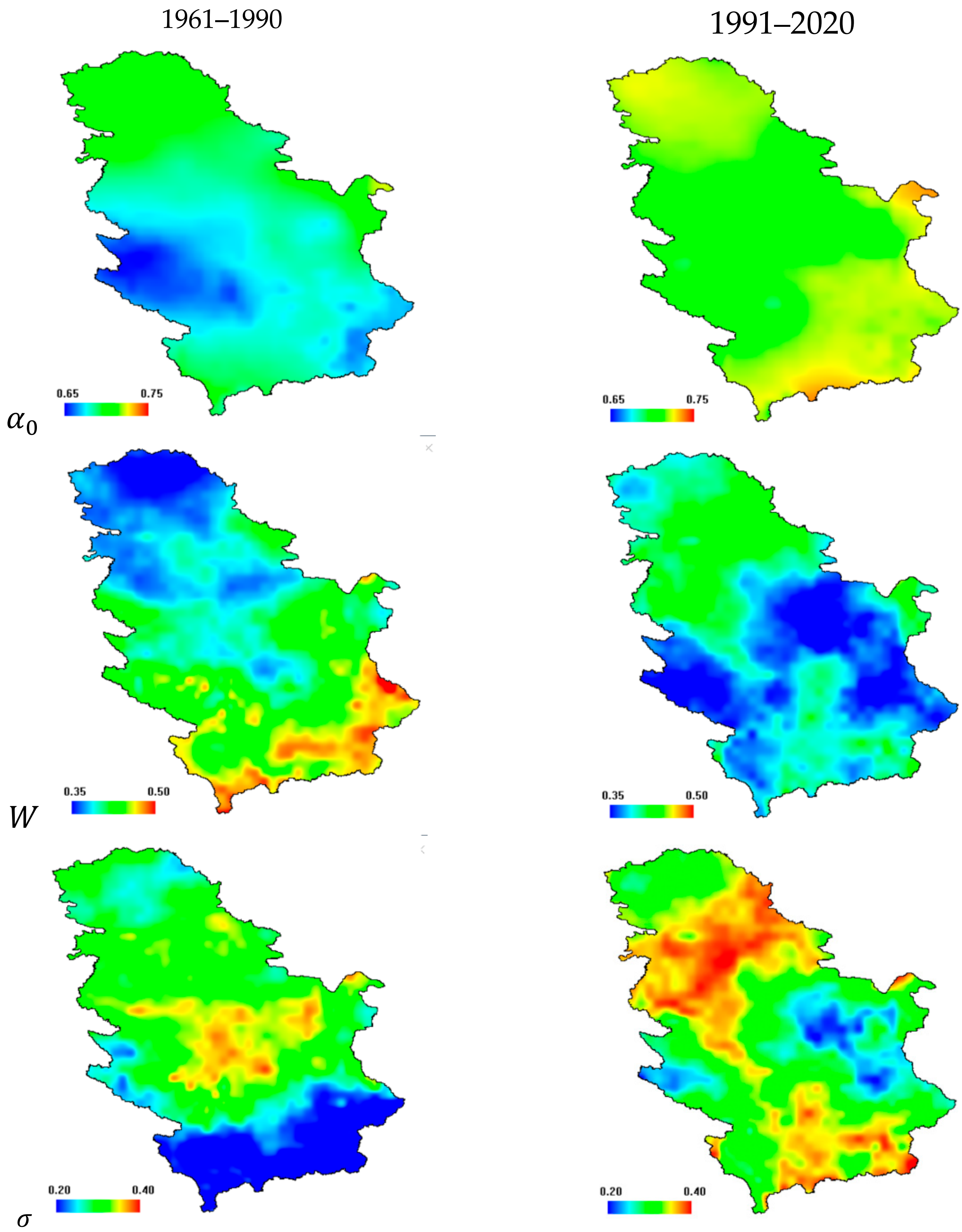

Figure 4. Spatial distribution of multifractal spectrum parameters: position of maximum α_0 (top row), spectrum width W (middle row) and skew parameter r (bottom row) of daily temperature series for the two considered periods: 1961–1990 (left column) and 1991–2020 (right column).

The frequency histograms of multifractal parameters shown in Figure 5 confirms that the distribution of parameters values is quite different in two periods: (i) for all parameters the distributions become narrower in the second period; (ii) the frequencies of higher values of α_0 and lower values of W increased in the second period indicating that overall the temperature fluctuations become more persistent with lower degree of multifractality; (iii) the distribution of skew parameter r changes from bimodal in the first period (due to the well separated southern region with lower values of r) to unimodal in the second period with increased frequencies of higher values, indicating the stronger dominance of small fluctuations.

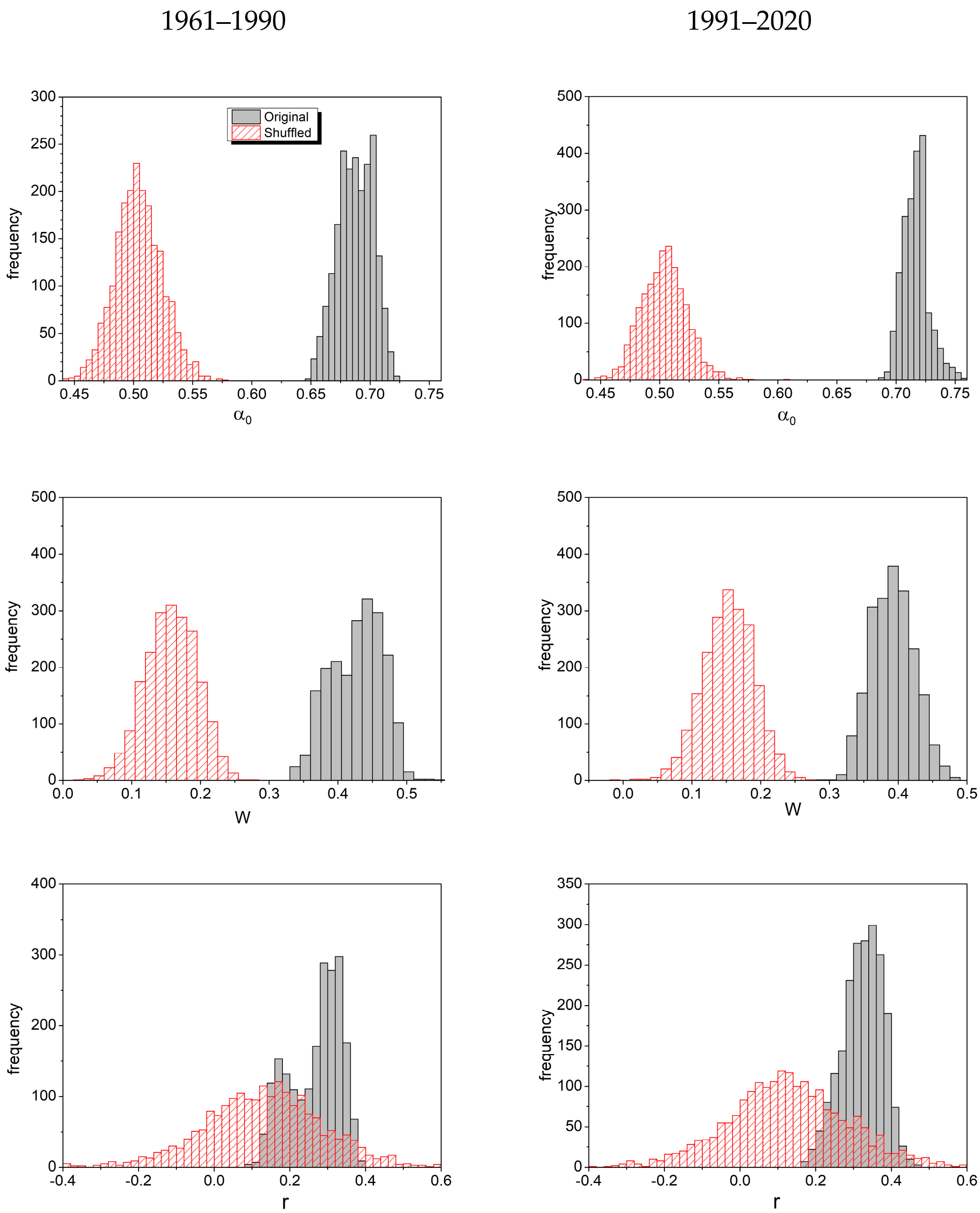

Figure 5. Histograms of the multifractal spectrum parameters: position of maximum α_0 (top row), spectrum width W (middle row), and skew parameter r (bottom row) of daily temperature series for the two considered periods: 1961–1990 (left column) and 1991–2020 (right column).

The histograms of shuffled series (shuffling was performed here only once, for each of the 1278 grid points) show the changes in multifractal parameters (the values of α_0 approaches 0.5, the width of the spectrum W decreases and the assimetry parameter r assumes both positive and negative values.

3.2. Comparison with Studies from Other Countries

Qualitatively, our results agree well with the results obtained for other European countries. Multifractality of air temperature series were found for Spain [58,59], Greece [60,61], Poland [62,63] and England [64] with the same specific features as for Serbia: persistent long-term correlations ($\alpha_0 > 0.5$) and the dominance of small fluctuations (right-skewed spectrum). Gos et al. [63] compared multifractal properties of air pressure, air temperature and wind speed in Poland, from ground base data (35 meteorological stations) and reanalysis gridded MERRA-2 dataset, for the period 2007–2016 on hourly and daily resolution. They found high similarity between multifractal parameters obtained from ground base and MERRA-2 data, for both hourly and daily series. For air temperature and air pressure the position of maximum of multifractal spectrum is strongly correlated with altitude: increases for air pressure and decreases for air temperature indicating that at higher altitudes the fluctuations of air temperature are less persistent. Our results also indicated that temperature fluctuations are less persistent in the mountainous regions. There are two studies that investigated possible influence of climate change. Gómez-Gómez et al. [58] analyzed four temperature variables (daily maximum, minimum, mean, and diurnal temperature range) by applying MFDFA on data recorded in 10 meteorological stations in Spain and compared multifractal spectrum parameters for two 30 years periods: 1960–1989 and 1990–2019. They found that all variables showed multifractal properties that changed in the second period and suggested that this was related to the climate change. For mean temperature, similar results for Serbia are obtained. In the second period the position of maximum of multifractal spectrum shifts to the right (the value of α_0 increases indicating stronger persistence) and the width of the spectrum decreased indicating lower degree of multifractality. Rahmani and Fattahi [64] investigated the influence of climate change on multifractal properties of precipitation and temperatures in central England (recorded in 11 stations) by applying MFDFA on daily and monthly data for two subperiods (1931–1989 and 1990–2019). They found that climate change induces shift in multifractal strength for all analyzed variables: on daily scale, the increase in multifractality for precipitation and maximum temperature and decrease in multifractality for minimum temperature, on monthly scale all variables display weaker multifractality which decreased for precipitation and increased for temperature in the second period. For Serbia the multifractality of daily mean temperature decreased in the second period in the regions with higher elevation.

Multifractal properties of air temperature were also found in other regions in world [17–19]. It is worth to compare our results with those of Da Silva et al. [18]. They applied MFDFA on daily temperature series recorded in 265 stations in Brazil during the period from 1990 to 2017. They found that all series showed multifractal properties with persistent long-term correlations and the dominance of large fluctuations. In southern region with higher elevation the temperature fluctuations display weaker persistency (lower α_0 values) and stronger multifractality (larger width W of multifractal spectrum). It is qualitatively similar as obtained for temperature series for Serbia in both considered periods: dominance of small fluctuations (right skewed $f(\alpha)$ spectrum) and weaker persistence (lower α_0 values) in mountainous regions.

4. Conclusions

The multifractality of air temperature in Serbia for two 30 years periods (1961–1990 and 1991–2020) was analyzed by applying Multifractal detrended fluctuation analysis (MFDFA) on high resolution daily gridded dataset. The obtained values of multifractal parameters (position of maximum α_0, width of the spectrum W and skew parameter r)

indicate that for both periods all series exhibit multifractal properties characterized by persistent long-term correlations, and dominance of small fluctuations.

By analyzing the spatial distribution of multifractal parameters for the first sub-period we found clear gradient of persistence and degree of multifractality in the direction from northern lowland to southern mountainous part of country: lower values of α_0 (weaker persistence) and higher values of W (stronger multifractality) in southern mountainous regions.

In the second period temperature series become more persistent (the values of α_0 increased in all regions, preserving the north-south gradient), while the change in W was not consistent: multifractality become stronger (larger W) in northern region and weaker (smaller W) in southern region.

The skew parameter r was positive in both periods, indicating the dominance of small fluctuations, that become stronger in the second period (the values of r increased in most of the country's area).

These changes in the values of multifractal parameters from first to second sub-period indicate that in the second period the underlying stochastic process that govern temperature fluctuations become more complex which could be attributed to climate change.

Similar results were found for Spain and England [58,64], indicating that multifractal analysis could be useful (along with classical statistical methods) in evaluation of climate change impact on air temperature fluctuations. By providing the information about the nature of underlying process (described by the parameters of multifractal spectrum) it could also be useful for validation of global and regional climate models, since a valid model should explain empirically detected scaling properties in observed data. Current results should be compared with model-generated data for spatial locations (longitude and latitude) that correspond to the locations of grid cells used in this work.

Author Contributions: Conceptualization, T.S. and B.S.; methodology, T.S. and B.S.; software, B.S.; validation, T.S., B.S., V.D. and I.T.; formal analysis, B.S., M.T. and I.L.; investigation, T.S., B.S., V.D. and I.T.; data curation, B.S., M.T. and I.L.; writing—original draft preparation, T.S., B.S., M.T. and I.L., V.D. and I.T.; writing—review and editing, T.S., B.S., V.D. and I.T.; visualization, B.S.; supervision, T.S.; project administration, T.S. and I.T. All authors have read and agreed to the published version of the manuscript.

Funding: This research received no external funding.

Institutional Review Board Statement: Not applicable.

Informed Consent Statement: Not applicable.

Data Availability Statement: The research data will be made available on request.

Acknowledgments: T.S and B.S acknowledge support of Brazilian agencies CAPES and CNPq (grants No 308782/2022-4 and 309499/2022-4). M.T., I.L., V.Dj. and I.T. acknowledge support of the Ministry of Education, Science and Technological Development of the Republic of Serbia, grant No. 451-03-47/2023-01/200162. We acknowledge the E-OBS dataset from the EU-FP6 project UERRA (https://www.uerra.eu, accessed on 26 June 2023) and the Copernicus Climate Change Service, and the data providers in the ECA&D project (https://www.ecad.eu, accessed on 26 June 2023).

Conflicts of Interest: The authors declare no conflict of interest. The funders had no role in the design of the study; in the collection, analyses, or interpretation of data; in the writing of the manuscript; or in the decision to publish the results.

References

1. Rind, D. Complexity and climate. *Science* **1999**, *284*, 105–107. [CrossRef]
2. Rodriguez-Iturbe, I.; Febres De Power, B.; Sharifi, M.B.; Georgakakos, K.P. Chaos in rainfall. *Water Resour.* **1989**, *25*, 1667–1675. [CrossRef]
3. Fuwape, I.A.; Ogunjo, S.T.; Oluyamo, S.S.; Rabiu, A.B. Spatial variation of deterministic chaos in mean daily temperature and rainfall over Nigeria. *Theor. Appl. Climatol.* **2017**, *130*, 119–132. [CrossRef]

4. Chang, T.P.; Ko, H.H.; Liu, F.J.; Chen, P.H.; Chang, Y.P.; Liang, Y.H.; Jang, H.Y.; Lin, T.C.; Chen, Y.H. Fractal dimension of wind speed time series. *Appl. Energy* **2012**, *93*, 742–749. [CrossRef]
5. Lovejoy, S.; Mandelbrot, B.B. Fractal properties of rain, and a fractal model. *Tellus A* **1985**, *37*, 209–232. [CrossRef]
6. Mali, P. Multifractal characterization of global temperature anomalies. *Theor. Appl. Climatol.* **2015**, *121*, 641–648. [CrossRef]
7. Kavasseri, R.G.; Nagarajan, R. A multifractal description of wind speed records. *Chaos Solitons Fractals* **2005**, *24*, 165–173. [CrossRef]
8. Kantelhardt, J.W.; Koscielny-Bunde, E.; Rybski, D.; Braun, P.; Bunde, A.; Havlin, S. Long-term persistence and multifractality of precipitation and river runoff records. *J. Geophys. Res.* **2006**, *111*, 1–13. [CrossRef]
9. Li, Q.; Zuntao, F. Permutation entropy and statistical complexity quantifier of nonstationarity effect in the vertical velocity records. *Phys. Rev. E Stat. Nonlinear Soft Matter Phys.* **2014**, *89*, 012905. [CrossRef]
10. Silva, A.S.A.D.; Barreto, I.D.D.C.; Cunha-Filho, M.; Menezes, R.S.C.; Stosic, B.; Stosic, T. Multiscale complexity analysis of rainfall in northeast Brazil. *Water* **2021**, *13*, 3213. [CrossRef]
11. Tongal, H.; Sivakumar, B. Transfer entropy coupled directed–weighted complex network analysis of rainfall dynamics. *Stoch. Environ. Res. Risk Assess.* **2022**, *36*, 851–867. [CrossRef]
12. Donges, J.F.; Zou, Y.; Marwan, N.; Kurths, J. Complex networks in climate dynamics: Comparing linear and nonlinear network construction methods. *Eur. Phys. J. Spec. Top.* **2009**, *174*, 157–179. [CrossRef]
13. Onyutha, C.; Rutkowska, A.; Nyeko-Ogiramoi, P.; Willems, P. How well do climate models reproduce variability in observed rainfall? A case study of the Lake Victoria basin considering CMIP3, CMIP5 and CORDEX simulations. *Stoch. Environ. Res. Risk Assess.* **2019**, *33*, 687–707. [CrossRef]
14. García-Marín, A.P.; Jiménez-Hornero, F.J.; Ayuso-Muñoz, J.L. Multifractal analysis as a tool for validating a rainfall model. *Hydrol. Process.* **2008**, *22*, 2672–2688. [CrossRef]
15. Deepthi, B.; Sivakumar, B. General circulation models for rainfall simulations: Performance assessment using complex networks. *Atmos. Res.* **2022**, *278*, 106333. [CrossRef]
16. Lovejoy, S.; Schertzer, D. *The Weather and Climate: Emergent Laws and Multifractal Cascades*, 2nd ed.; Cambridge University Press: Cambridge, UK, 2018; 480p.
17. Jiang, L.; Zhang, J.; Liu, X.; Li, F. Multi-fractal scaling comparison of the air temperature and the surface temperature over China. *Phys. A Stat. Mech. Appl.* **2016**, *462*, 783–792. [CrossRef]
18. Da Silva, H.S.; Silva, J.R.S.; Stosic, T. Multifractal analysis of air temperature in Brazil. *Phys. A Stat. Mech. Appl.* **2020**, *549*, 124333. [CrossRef]
19. Akinsusi, J.; Ogunjo, S.; Fuwape, I. Nonlinear dynamics and multifractal analysis of minimum–maximum temperature and solar radiation over Lagos State, Nigeria. *Acta Geophys.* **2022**, *70*, 2171–2178. [CrossRef]
20. Adarsh, S.; Nourani, V.; Archana, D.S.; Dharan, D.S. Multifractal description of daily rainfall fields over India. *J. Hydrol.* **2020**, *586*, 124913. [CrossRef]
21. Gómez-Gómez, J.; Carmona-Cabezas, R.; Sánchez-López, E.; de Ravé, E.G.; Jiménez-Hornero, F.J. Multifractal fluctuations of the precipitation in Spain (1960–2019). *Chaos Solitons Fractals* **2022**, *157*, 111909. [CrossRef]
22. De Lima, M.I.P.; Grasman, J. Multifractal analysis of 15-min and daily rainfall from a semi-arid region in Portugal. *J. Hydrol.* **1999**, *220*, 1–11. [CrossRef]
23. Tan, X.; Gan, T.Y. Multifractality of Canadian precipitation and streamflow. *Int. J. Climatol.* **2017**, *37*, 1221–1236. [CrossRef]
24. Liu, Z.; Xu, J.; Chen, Z.; Nie, Q.; Wei, C. Multifractal and long memory of humidity process in the Tarim River Basin. *Stoch. Environ. Res. Risk Assess.* **2014**, *28*, 1383–1400. [CrossRef]
25. Garcia-Marin, A.P.; Estévez, J.; Jiménez-Hornero, F.J.; Ayuso-Muñoz, J.L. Multifractal analysis of validated wind speed time series. *Chaos* **2013**, *23*, 013133. [CrossRef] [PubMed]
26. Laib, M.; Golay, J.; Telesca, L.; Kanevski, M. Multifractal analysis of the time series of daily means of wind speed in complex regions. *Chaos Solitons Fractals* **2018**, *109*, 118–127. [CrossRef]
27. Dos Santos, F.S.; do Nascimento, K.K.F.; da Silva Jale, J.; Stosic, T.; Marinho, M.H.; Ferreira, T.A. Mixture distribution and multifractal analysis applied to wind speed in the Brazilian Northeast region. *Chaos Solitons Fractals* **2021**, *144*, 110651. [CrossRef]
28. Zeng, Z.; Yang, H.; Zhao, R.; Meng, J. Nonlinear characteristics of observed solar radiation data. *Sol. Energy* **2013**, *87*, 204–218. [CrossRef]
29. Dos Santos, F.S.; Do Nascimento, K.K.F.; Jale, J.S.; Xavier Júnior, S.F.A.; Ferreira, T.A. Multifractal Analysis of Solar Radiation in the Northeastern Region of Brazil. *Fractals* **2023**, *31*, 2350025. [CrossRef]
30. Maruyama, F. The relation among the solar activity, the total ozone, QBO, NAO, and ENSO by wavelet-based multifractal analysis. *J. Appl. Math. Phys.* **2018**, *6*, 1301–1314. [CrossRef]
31. Varotsos, C.A.; Cracknell, A.P.; Efstathiou, M.N. The global signature of the el Niño/La Niña southern oscillation. *Int. J. Remote Sens.* **2018**, *39*, 5965–5977. [CrossRef]
32. Folland, C.K.; Karl, T.R.; Christy, J.R.; Clarke, R.A.; Gruza, G.V.; Jouzel, J.; Mann, M.E.; Oerlemans, J.; Salinger, M.J.; Wang, S.W. Observed climate variability and change. In *Climate Change 2001*; Cambridge University Press: New York, NY, USA, 2001; pp. 99–181.

33. Manabe, S. Role of greenhouse gas in climate change. *Tellus A* **2019**, *71*, 1620078. [CrossRef]
34. Mikhaylov, A.; Moiseev, N.; Aleshin, K.; Burkhardt, T. Global climate change and greenhouse effect. *Entrep. Sustain. Issues* **2020**, *7*, 2897–2913. [CrossRef] [PubMed]
35. Kantelhardt, J.W.; Zschiegner, S.A.; Koscielny-Bunde, E.; Havlin, S.; Bunde, A.; Stanley, H.E. Multifractal detrended fluctuation analysis of nonstationary time series. *Phys. A Stat. Mech. Appl.* **2002**, *316*, 87–114. [CrossRef]
36. Bajat, B.; Blagojević, D.; Kilibarda, M.; Luković, J.; Tošić, I. Spatial analysis of the temperature trends in Serbia during the period 1961–2010. *Theor. Appl. Climatol.* **2015**, *121*, 289–301. [CrossRef]
37. Ruml, M.; Gregorić, E.; Vujadinović, M.; Radovanović, S.; Matović, G.; Vuković, A.; Počuča, V.; Stojičić, D. Observed changes of temperature extremes in Serbia over the period 1961−2010. *Atmos. Res.* **2017**, *183*, 26–41. [CrossRef]
38. Malinović-Milićčević, S.; Radovanović, M.M.; Stanojević, G.; Milovanović, B. Recent changes in Serbian climate extreme indices from 1961 to 2010. *Theor. Appl. Climatol.* **2016**, *124*, 1089–1098. [CrossRef]
39. Unkašević, M.; Tošić, I. Trends in temperature indices over Serbia: Relationships to large-scale circulation patterns. *Int. J Climatol.* **2013**, *33*, 3152–3161. [CrossRef]
40. Tošić, I.; Tošić, M.; Lazić, I.; Aleksandrov, N.; Putniković, S.; Djurdjević, V. Spatio-temporal changes in the mean and extreme temperature indices for Serbia. *Int. J Climatol.* **2023**, *43*, 2391–2410. [CrossRef]
41. Unkašević, M.; Tošić, I. Seasonal analysis of cold and heat waves in Serbia during the period 1949–2012. *Theor. Appl. Climatol.* **2015**, *120*, 29–40. [CrossRef]
42. Milovanović, B.; Schubert, S.; Radovanović, M.; Vakanjac, V.R.; Schneider, C. Projected changes in air temperature, precipitation and aridity in Serbia in the 21st century. *Int. J Climatol.* **2022**, *42*, 1985–2003. [CrossRef]
43. Cornes, R.; van der Schrier, G.; van den Besselaar, E.J.M.; Jones, P.D. An Ensemble Version of the E-OBS Temperature and Precipitation Datasets. *J. Geophys. Res. Atmos.* **2018**, *123*, 9391–9409. [CrossRef]
44. Muzy, J.F.; Bacry, E.; Arneodo, A. Wavelets and multifractal formalism for singular signals: Application to turbulence data. *Phys. Rev. Lett.* **1991**, *67*, 3515–3518. [CrossRef]
45. Gu, G.-F.; Zhou, W.-X. Detrending moving average algorithm for multifractals. *Phys. Rev. E* **2010**, *82*, 011136. [CrossRef]
46. Oswiecimka, P.; Kwapien, J.; Drozd, S. Wavelet versus detrended fluctuation analysis of multifractal structures. *Phys. Rev. E* **2006**, *74*, 016103. [CrossRef] [PubMed]
47. Maity, A.K.; Pratihar, R.; Mitra, A.; Dey, S.; Agrawal, V.; Sanyal, S.; Banerjee, A.; Sengupta, R.; Ghosh, D. Multifractal detrended fluctuation analysis of alpha and theta EEG rhythms with musical stimuli. *Chaos Solitons Fractals* **2015**, *81*, 52–67. [CrossRef]
48. Aggarwal, S.K.; Lovallo, M.; Khan, P.K.; Rastogi, B.K.; Telesca, L. Multifractal detrended fluctuation analysis of magnitude series of seismicity of Kachchh region, Western India. *Phys. A Stat. Mech. Appl.* **2015**, *426*, 56–62. [CrossRef]
49. Balkissoon, S.; Fox, N.; Lupo, A. Fractal characteristics of tall tower wind speeds in Missouri. *Renew. Energy* **2020**, *154*, 1346–1356. [CrossRef]
50. Wu, Y.; He, Y.; Wu, M.; Lu, C.; Gao, S.; Xu, Y. Multifractality and cross-correlation analysis of streamflow and sediment fluctuation at the apex of the Pearl River Delta. *Sci. Rep.* **2018**, *8*, 16553. [CrossRef]
51. Wątorek, M.; Drożdż, S.; Kwapień, J.; Minati, L.; Oświęcimka, P.; Stanuszek, M. Multiscale characteristics of the emerging global cryptocurrency market. *Phys. Rep.* **2021**, *901*, 1–82. [CrossRef]
52. Hurst, H. Long-term storage capacity of tanks. In Proceedings of the American Society of Civil Engineers; American Society of Civil Engineers: Reston, VA, USA, 1951; Volume 116, pp. 770–799.
53. Mandelbrot, B.B. *Fractal Geometry of Nature*; Times Book: New York, NY, USA, 1982; 480p.
54. Shimizu, Y.U.; Thurner, S.; Ehrenberger, K. Multifractal spectra as a measure of complexity in human posture. *Fractals* **2002**, *10*, 103–116. [CrossRef]
55. Stosic, T.; Nejad, S.A.; Stosic, B. Multifractal analysis of Brazilian agricultural market. *Fractals* **2020**, *28*, 2050076. [CrossRef]
56. Putniković, S.; Tošić, I.; Đurđević, V. Circulation weather types and their influence on precipitation in Serbia. *Meteor. Atmos. Phys.* **2016**, *128*, 649–662. [CrossRef]
57. Mimić, G.; Mihailović, D.T.; Kapor, D. Complexity analysis of the air temperature and the precipitation time series in Serbia. *Theor. Appl. Climatol.* **2017**, *127*, 891–898. [CrossRef]
58. Gómez-Gómez, J.; Carmona-Cabezas, R.; Ariza-Villaverde, A.B.; de Ravé, E.G.; Jiménez-Hornero, F.J. Multifractal detrended fluctuation analysis of temperature in Spain (1960–2019). *Phys. A Stat. Mech. Appl.* **2021**, *578*, 126118. [CrossRef]
59. Burgueño, A.; Lana, X.; Serra, C.; Martínez, M.D. Daily extreme temperature multifractals in Catalonia (NE Spain). *Phys. Lett. A* **2014**, *378*, 874–885. [CrossRef]
60. Kalamaras, N.; Tzanis, C.G.; Deligiorgi, D.; Philippopoulos, K.; Koutsogiannis, I. Distribution of Air Temperature Multifractal Characteristics Over Greece. *Atmosphere* **2019**, *10*, 45. [CrossRef]
61. Philippopoulos, K.; Kalamaras, N.; Tzanis, C.G.; Deligiorgi, D.; Koutsogiannis, I. Multifractal detrended fluctuation analysis of temperature reanalysis data over Greece. *Atmosphere* **2019**, *10*, 336. [CrossRef]
62. Baranowski, P.; Gos, M.; Krzyszczak, J.; Siwek, K.; Kieliszek, A.; Tkaczyk, P. Multifractality of meteorological time series for Poland on the base of MERRA-2 data. *Chaos Solitons Fractals* **2019**, *127*, 318–333. [CrossRef]

63. Gos, M.; Baranowski, P.; Krzyszczak, J.; Kieliszek, A.; Siwek, K. Dynamics of meteorological time series on the base of ground measurements and retrospective data from MERRA-2 for Poland. *Int. J. Climatol.* **2021**, *41*, E1531–E1552. [CrossRef]
64. Rahmani, F.; Fattahi, M.H. Climate change-induced influences on the nonlinear dynamic patterns of precipitation and temperatures (case study: Central England). *Theor. Appl. Climatol.* **2023**, *152*, 1147–1158. [CrossRef]